







$a_p(526)$ , was a near-negligible fraction of  $c_p(526)$  ( $\sim 4 \pm 1\%$ ), such that  $c_p \approx b_p$ . This is true across most of the visible spectrum, except near the phytoplankton absorption maximum in the blue ( $\sim 440$  nm) and is noteworthy for comparison with historical relationships which may use  $b_p$  or  $c_p$ , whereas we will consider them equivalent (see also [19]). Figure 1A shows  $b_{bp}(526)$  plotted versus  $c_p(526)$  for the four cruises. The number of data points ( $N \sim 10^5$ ) requires a bivariate histogram to see underlying trends. A weighted linear least squares regression applied to all data yields a slope of  $(9.1 \pm 0.4) \times 10^{-3}$  and an intercept of  $(2.0 \pm 0.1) \times 10^{-4} \text{ m}^{-1}$  ( $r^2 = 0.92$ , uncertainties estimated from 1000 bootstrap samples). The resulting backscattering ratios (dimensionless) are shown in Fig. 1B and can be described by a median value  $\pm$  the percentile range equivalent to a standard deviation around a normal distribution. For the Equatorial Pacific, North Atlantic, Mediterranean Sea, and Northeast Pacific these values are  $0.011 \pm 0.001$ ,  $0.010 \pm 0.002$ ,  $0.010 \pm 0.002$ , and  $0.012 \pm 0.003$  respectively. The full range of the four data sets, described by the 5th-95th percentile range, is 0.007-0.015.

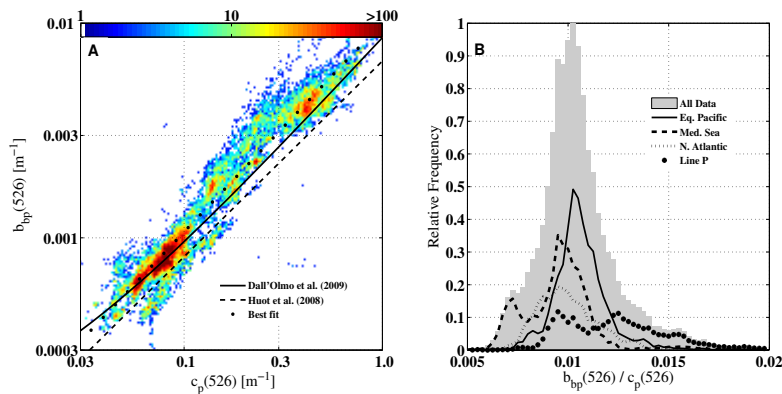


Fig. 1. **A.** Relationship between backscattering ( $b_{bp}$ ) and beam attenuation ( $c_p$ ) at 526 nm (colors indicate number of observations at each  $b_{bp}, c_p$  pair). “Best fit” line is calculated from weighted linear regression of 2D histogram with weights assigned as the square of the number of points found in each bin. Relationship of Huot et al. [20] (dashed line) was derived from equivalence of their Eqs. (8) and 9, while that of Dall’Olmo et al. [12] (solid line) was derived from the Equatorial Pacific data set alone. **B.** Distributions of backscattering ratio ( $b_{bp}: c_p$ ) at 526 nm for each data set and for all data combined. Histograms have been normalized to the total number of observations ( $N \sim 10^5$ ).

Figures 2A and 2C show the two scattering indices,  $c_p$  and  $b_{bp}$ , as a function of chlorophyll concentration. Particle attenuation ( $c_p$ ) and scattering ( $b_p$ ) have been empirically related to  $Chl$  for a long time and several relationships can be found in the literature [19–21]. The typical open ocean standard is taken from [19] which provided expressions for different vertical layers, and for a few different regions of the ocean (e.g., the North Atlantic). Data presented here match the expected values of  $c_p$  from [19] at low  $Chl$ , but deviate significantly at higher  $Chl$ , which in our data set come almost exclusively from the North Atlantic. However, the fit derived by Loisel and Morel [19] when their own North Atlantic data were included is in good agreement with data presented here (normalized median bias (NMB),  $X_{\text{measured}} - X_{\text{modeled}} / X_{\text{measured}} * 100 \sim 11\%$ , consistent with the difference in acceptance angles of the instruments used in the two studies). Loisel and Morel [19] assumed that this increased scattering per unit chlorophyll observed when the North Atlantic data were included was due to the presence of coccolithophorids and/or detached liths. On the contrary, in our data set, coccolithophorids and their liths were not observed in flow cytometric and microscopic measurements [22]. Also, the backscattering ratio, which was unavailable to Loisel and Morel [19], is not significantly higher in the North Atlantic data presented here than in the other data sets (Fig. 1B). The backscattering of coccolithophorids and their liths is a hallmark of their presence and is the basis for their detection in satellite ocean color data [23].

Similarly,  $b_{bp}(526)$  from the North Atlantic is significantly higher than expected based on the relationships of Morel and Maritorena [21], while agreement improves at lower chlorophyll concentrations (Fig. 2C). The updated relationship of Huot et al. [20] also agrees better at lower  $Chl$ , but still underestimates our observations of  $b_{bp}(526)$  at moderate to high chlorophyll concentrations (normalized median difference = 42% when  $Chl > 1 \text{ mg m}^{-3}$ ). It is these higher values for which we have direct validation (see Discussion and Fig. 3C) and therefore, disagreement with previously published relationships in the high  $Chl$  range (1-10  $\text{mg m}^{-3}$ ) may be related to the paucity of high  $Chl$  open ocean observations in previous data sets rather than uniqueness in the data presented here.

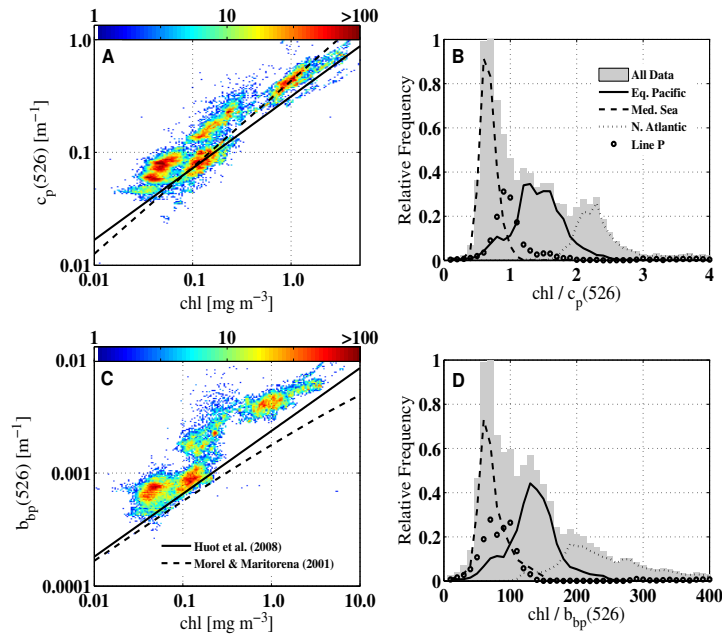


Fig. 2. Particle beam attenuation ( $c_p$ ) and backscattering ( $b_{bp}$ ) at 526 nm as a function of chlorophyll ( $Chl$ ).  $Chl$  ( $\text{mg m}^{-3}$ ) is estimated using an absorption line height approach [18] where  $Chl = (a_p(676) - (0.6a_p(650) + 0.4a_p(714))) / a^*_{Chl}$  and  $a^*_{Chl} = 0.014 \text{ m}^2 \text{ mg}^{-1}$ ; **A**,  $c_p(526)$  versus  $Chl$ . Solid black line is the model of Loisel and Morel [19], dashed black line is [19] when including their North Atlantic data. Loisel and Morel [19] relationships were extrapolated to 526 nm (from 660 nm) using a spectral slope of  $\lambda^{-1}$ . **B**, distribution of the ratio  $Chl:c_p$  for each cruise and all data combined; **C**,  $b_{bp}(526)$  versus  $Chl$ . Solid black line is the model of Huot et al. and dashed black line is model of Morel and Maritorena [21]. **D**, distribution of the ratio  $Chl:b_{bp}$  for each cruise and all data combined.

#### 4. Discussion

The accuracy and precision of the measurements presented here can be evaluated with a limited number of overlapping measurements for  $chl$ ,  $c_p$ , and  $b_{bp}$ . Discrete matchups with HPLC-derived  $Chl$  are in excellent agreement (Fig. 3A), median bias in ACs-based  $Chl$  estimates is  $-0.002 \pm 0.067 \text{ mg m}^{-3}$  (NMB =  $-2\% \pm 18\%$ ). Similar matchups of  $c_p$  with transmissometers mounted on the CTDs of each cruise also compare well, median bias is  $0.0001 \pm 0.031 \text{ m}^{-1}$  (NMB =  $-0.2\% \pm 11.4\%$ ) (Fig. 3B). Comparisons with independent  $b_{bp}$  estimates were only available for the subset of data taken from the North Atlantic and are shown in Fig. 3C. One caveat is that the sensors, although identical, measured at different wavelengths (526 and 700 nm for the underway and CTD-mounted instruments, respectively) and it might be expected *a priori* that  $b_{bp}$  values be slightly higher at 526 nm than 700 nm depending upon the slope of the backscattering spectrum. However, in highly productive

regions such as the North Atlantic, we can expect the backscattering spectrum to be relatively flat (slope $\sim$ 0, e.g., [24,25]) and spectral differences to be minimal. The median ratio of the underway to CTD  $b_{bp}$  values is  $1.04 \pm 0.07$  suggesting that underway  $b_{bp}$  values are  $\sim$ 4% higher. Thus, the values we present are robust and have no significant biases.

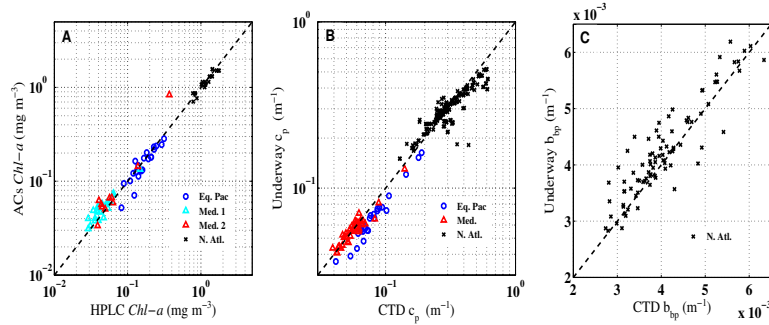


Fig. 3. Chlorophyll ( $Chl$ ), particle attenuation ( $c_p$ ) and backscattering ( $b_{bp}$ ) matchups between continuous flow through measurements and discrete *in situ* measurements. **A.** HPLC total  $Chl-a$  ( $Chl a + divinyl Chl a + Chlorophyllide a$ ) plotted versus simultaneous AC-s estimates made using absorption line height method (see previous figure caption).  $N = 99$ ,  $r^2 = 0.94$ . **B.** Near surface  $c_p$  (depth  $< 5$  meters) calculated from CTD-mounted instruments on each cruise plotted versus simultaneous measurements with similar instrument (WETLabs C-Star, 660nm) made on continuous flowing seawater from ship's intake.  $N = 262$ ,  $r^2 = 0.91$ . **C.** CTD-mounted  $b_{bp}$  estimates (depth  $< 5$ m) versus underway estimates,  $N = 89$ ,  $r^2 = 0.83$ . Dashed line in each represents 1:1 line.

Most studies of the backscattering ratio to date have focused on contrasting the full range of  $b_{bp}:c_p$  from surface open ocean to coastal waters to bottom boundary layers [16,26,27]. Huot et al. [20] reported the first comprehensive set of  $b_p$ ,  $b_{bp}$ , and  $Chl$  measurements in the open ocean and found a median  $b_{bp}:c_p$  at 532nm  $\sim$ 0.006 with no obvious  $Chl$  dependence. However, the same quantity at neighboring wavelengths (510 and 589 nm) was also measured by [17] and found to be higher ( $b_{bp}:c_p \sim$ 0.01). Here we greatly expand the range, both dynamic and geographic, and number of measurements ( $N \sim 10^5$  compared to  $N \sim 10^2$ ) to examine the robustness of these findings. While our conclusions are somewhat similar, we find a median value ( $b_{bp}:c_p \sim$ 0.01) which is remarkably conserved across very different oceanic environments and in good agreement with Stramski et al. [17] and Whitmire et al [16]. Although it is impossible to determine the exact reason for this observation with current data, one intriguing hypothesis is that phytoplankton-sized particles contribute significantly to both  $c_p$  and  $b_{bp}$  [9,10,12]. Indeed, for much of the ocean,  $c_p$  variability reflects phytoplankton biomass [9,10]. Given the universal coherence between  $c_p$  and  $b_{bp}$  found here, it would appear that  $b_{bp}$  conveys similar information. Arguments against this possibility rely on [Mie] theoretical results which have documented shortcomings in their treatment of phytoplankton attributes [28]. Nevertheless, if this observation holds true, utilization of  $b_{bp}$  as a proxy for phytoplankton biomass and the  $Chl:b_{bp}$  ratio as a phytoplankton physiological index should be possible [13,14].

One point of departure between these data and those previously reported (e.g., [19,20]) is the seemingly poor relationship between  $Chl$  and  $c_p$  or  $b_{bp}$ . This is in contrast to the usual presumption that the two scattering indices smoothly vary as a function of  $Chl$ , albeit with some degree of noise (c.f., large amount of scatter in Fig. 3A of [19]). Although the first order dependence is indeed due to biomass (and thus  $Chl$  by association), there are several reasons to expect significant dispersion in either of these relationships. Differences in cell size, photoacclimation state, and nutrient limitation (particularly with respect to iron) will all exert control on cellular chlorophyll content, and thus, the apparent chlorophyll per unit scattering (or backscattering). The collective data set presented here spans a large gradient in each of these factors and a simple qualitative accounting due to each provides insight to the individual  $Chl:c_p$  distributions seen in Fig. 2B. For example, the oligotrophic Mediterranean Sea data can

be characterized as *Synechococcus* and *Prochlorococcus* dominated (from HPLC data, not shown) which are high-light and low-nutrient acclimated. The small size of these phytoplankters (cell diameter  $\leq 1\mu\text{m}$ ) and their subtropical, high light environment give them the smallest  $Chl:c_p$  ratio (Fig. 2B). In contrast, the springtime North Atlantic data were collected under diatom-rich conditions (HPLC data, not shown) having typical sizes from  $\sim 10\mu\text{m}$  to greater than  $100\mu\text{m}$ . Acclimation irradiances were presumably quite low based on the time of year (May), high latitude ( $\sim 62^\circ\text{N}$ ) and moderately deep mixed layer depths ( $\sim 40\text{--}50\text{ m}$ , not shown). The combined effects of these growth conditions result in the highest  $Chl:c_p$  values observed (Fig. 2B). Last, we know that the Equatorial Pacific and subarctic North Pacific are chronically iron limited regions, while the North Atlantic and Mediterranean are generally not, making iron effects on intracellular *Chl* and growth an important consideration also.

In summary, we show that variance around the  $b_{bp}:c_p$  ratio over its entire range is much smaller than that of the  $Chl:c_p$  or  $Chl:b_{bp}$  ratio, suggesting that the two scattering indices,  $c_p$  and  $b_{bp}$ , are better related to one another than either are to the traditional pigment biomass index, *Chl*. The quality and unprecedented number of observations reported here gives a fresh view of how these properties are related (or not) to one another. Unfortunately, we do not currently have all the data required to confirm reasons for the coherence of  $b_{bp}$  and  $c_p$ , nor the variability in  $Chl:c_p$  and  $Chl:b_{bp}$  ratios. However, expected variability in these ratios due to environmental factors is consistent with their observed distributions. It follows that relationships between  $c_p$  and phytoplankton biomass [8], or between  $Chl:c_p$  and phytoplankton physiological indices [9], can be conceptually extended to the use of  $b_{bp}$ . This finding lends support to the use of satellite-derived *Chl* and  $b_{bp}$  for investigation of phytoplankton biomass and physiology and broadens the applications of existing ocean color retrievals. Ongoing validation in different oceanic environments, particularly the oligotrophic subtropical gyres, is nevertheless, desirable.

### Acknowledgements

This work was funded by NASA grant number NNX08AK70G and NNG05GD18G. The authors would like to thank Josephine Ras and Mary Jane Perry for providing validation data used in Fig. 3. We would also like to thank the captains, crews, and scientific participants aboard the cruises used in this work. The BOUM cruise in the Mediterranean Sea was co-funded by the French national LEFE-CYBER program (INSU CNRS) and the European IP SESAME.